Solitary wave impact on a vertical wall

Atle Jensen

Department of Mathematics, University of Oslo,

Po. Box 1053, NO-0316, Oslo, Norway.

May 14, 2018

Wave impact on a vertical wall has been investigated in a physical - and numerical wave tank. Two different impact phenomena were explored. A flip-through, where the front face of the wave was moving rapidly vertical due to a jet and a case with a very steep wave were generated in a wave tank. In the latter, the front was almost vertical and the measured pressure at impact was 60% higher than the flip-through event.

Both kinematics and pressures were measured and compared with numerical simulations. Similar features were seen in both experiments and simulations. Maximum pressure is found when a vertical front is violently impacting on a vertical wall. A pronounced double pressure peak is observed in the pressure measurements due to the impact and rundown process.

1 Introduction

Breaking waves is a topic of hydrodynamic wave theory for which our insight is still very limited. Qualitative description and classification are found in, for instance, Cokelet (1977); Peregrine (1983) and formation of plungers have been simulated since 1976 (Longuet-Higgins & Cokelet (1976)), but a number of aspects and applications for breaking waves still await proper analysis. In mid ocean breaking waves are important for momentum transfer from wind to ocean currents as well as mixing of the surface layers. From an engineering point of view plunging breakers and extremely steep waves may present extreme loads on structures and vessels, see Peregrine (2003).

Violent impact on structures can cause damage in coastal areas and in deep water. The pressure forces from breaking waves can be large when they impact with structures, for example breakwaters, vessels and offshore wind turbines. There are numerous of studies conducted with this topic and a recent investigation was published by Plumerault *et al.* (2012). They analyzed the role of the presence of air on the impact of braking waves on a vertical wall. Others have also studied this problem, see e.g. Chan & Melville (1988) and Hattori *et al.* (1994). The SPH method has been used extensively during the last decade to model breaking wave impact, see e.g. Dao *et al.* (2013), Guilcher *et al.* (2012) and Guilcher *et al.* (2010).

Oumeraci *et al.* (1993) performed experiments where they generated different types of breaking waves and measured the loads on vertical structures. A more recent and similar study is by Bullock *et al.* (2007). They investigated four different types of impact and discussed how aeration changed the impact.

There exist several classifications of waves impacting structures; flip-through, vertical wave front and plunging breakers where air is captured between the wall and water. The flip-through phenomenon is defined as, in e.g. Peregrine (2003), a high-speed, vertical jet which emerges from the toe of the wave before impact. Lugni *et al.* (2006) studied the flip-through in great detail, measuring the kinematics and dynamics of the waves when they impact. A comprehensive study by Scolan (2010) investigated this phenomenon using potential theory without surface tension. Hattori *et al.* (1994) studied several of the mentioned phenomena with pressure gauges and high speed video. The work by Cuomo *et al.* (2010) included experiments in a large scale flume. Irregular waves were generated, wave loads were measured and scale effects were studied. The wave forces were compared with existing prediction methods and also a new prediction formulae was presented. They also include a very nice literature review of related investigations, both experimental and numerical. Kimmoun *et al.* (2009) have conducted a very similar set of experiments to the present study. However, they used a flexible vertical wall that were exposed to breaking waves.

In Jensen *et al.* (2003), the dynamics of incident solitary waves on the verge of onshore plunging, on a 10.54° slope, were investigated with the PIV technique. Among other things, acceleration distributions leading to reversal of breaking in overhanging waves were reported. In Jensen *et al.* (2005) another set of experiments with runup of solitary waves on a 7.18° slope was studied. The velocity and acceleration distribution in massive onshore plungers are measured with PIV and computed by a VOF technique. This investigation aimed to recognize conditions leading to extreme runup and onshore impact of tsunamis and swells.

The present study employs the same incidents waves as Jensen *et al.* (2005), but the inclination of the beach is lowered to 5.1° as in Smith *et al.* (2017). Waves may now develop large, but well defined, plungers as opposed to the collapsing breaker that was reported in Jensen *et al.* (2005). A surface-piercing vertical plate is mounted at the beach. The aim of the these experiments is to measure the time evolution of the pressure, which is measured at the wall with three probes, and wave kinematics. Special attention is given to the rundown process where a second peak in the pressure recordings is observed and also reported by Oumeraci *et al.* (1993). Experiments with breaking waves only and impact on a cylinder were also conducted. These results are reported in Mo *et al.* (2013) together with numerical simulation. The experimental data were also used recently in Chella *et al.* (2017), validating a numerical model (codename REEF3D).

2 Methods

2.1 Experimental setup

All experiments were conducted in the wave flume at the Hydrodynamics laboratory, University of Oslo. The wave flume is 1 m high, 0.5 m wide and 25 m long. At one end of the flume solitary waves were generated by a hydraulic piston attached to a vertical paddle and an iteration technique was used to generate a pure solitary wave, see Jensen *et al.* (2005) for more details. All experiments were repeated three times. The water depth was $h = 0.205$ m for all runs. Opposite to the wave paddle, a beach was mounted with an inclination of 5.1° at a distance of 5.2 m from the mean position of the wave maker to the leading edge of the beach. The experimental setup is shown in Figure 1. Two different wall positions (W1 and W2 in Figure 1) were used in the experiments. Wall 1 and wall 2 were located at 0.0237 m and 0.037 m, respectively, upstream from the still water level on the beach. These walls were rigidly mounted on to steel frames connected to the wave tank structure to minimize any motions of the wall due to the impact of the solitary wave.

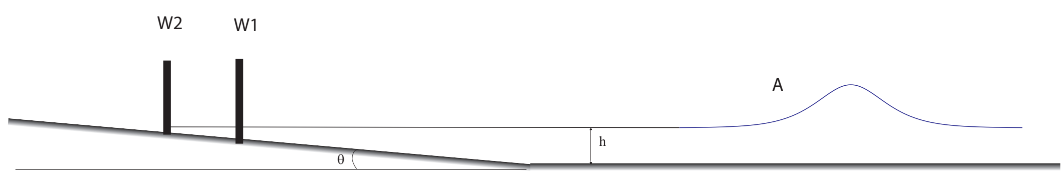

Figure 1: Sketch of the flume with the location of the two walls. Only one wall was used at a time for each experiment.

2.2 Particle image velocimetry

Velocities were measured using particle image velocimetry (PIV). Velocities were calculated using a cross-correlation method from subsequent images obtained with a high speed video camera. Passive particles of diameter 50 μm were added to the flow and illuminated using a Nd:YLF laser. The data acquisition rate for the measurements were for most cases 1000 fps. Three pressure gauges with a sampling rate of 300 Hz were flush mounted on the wall with a vertical spacing of 2.5 cm from the beach.

The surface elevation of the incident wave was measured by an acoustic wave gauge when the wave traveled in finite depth. Figure 2 shows a solitary wave measured by this method. Free surface profiles are also extracted from digital images obtained with the high speed video camera to acquire a spatial profile of the solitary wave.

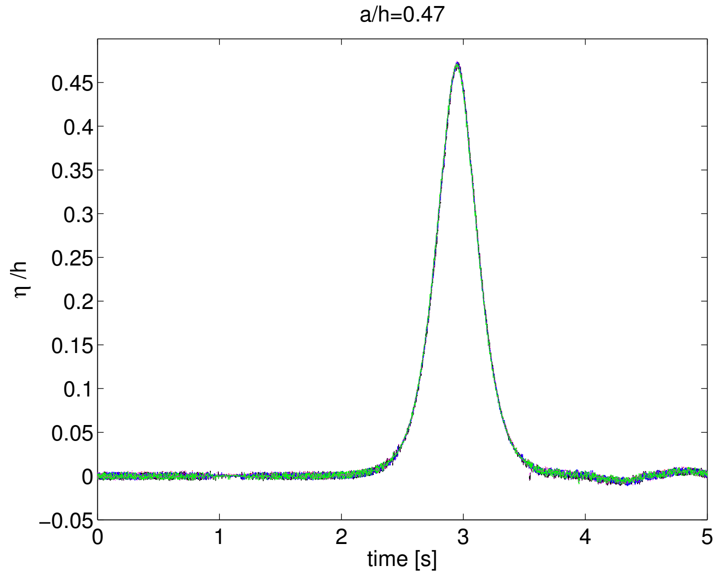

Figure 2: Free surface elevation of the incident wave, $A/h = 0.47$.

Experimental data were collected with one data acquisition card and trigged with the same time base. This is to secure that there is no phase lag between the different instruments used in this investigation.

2.3 Numerical experiment

All numerical simulations were performed with a incompressible Navier-Stokes model with codename NS3. The basic spatial and temporal discretization of NS3 follows Mayer *et al.* (1998), Mayer & Madsen (2000) and Kawamura *et al.* (2002), using projection and a finite volume method with cell-centered variable layout on moving general curvilinear multi-block grids using the Arbitrary Lagrangian Eulerian (ALE) approach. Numerical time integration of the momentum equation is performed to second order accuracy. To describe the free surface geometry, the VOF methodology of Hirt & Nichols (1981) is applied. The viscous term is neglected and only the Euler equation is solved. See also Jensen *et al.* (2005) for more information. The motion of the wavemaker was measured with high accuracy and used as input to the numerical wave tank. Some preliminary simulations without walls were performed to find the optimal positions of the two walls. Two cases were wanted; a gentle collision and a more violent impact with as little air captured in the wave as possible. Therefore, an incompressible solver can be used to simulate these events.

3 Results

The same solitary wave with nondimensionalized amplitude $A/h = 0.47$, where A is the amplitude of the solitary wave and h is the depth, was used for the impact with the wall for both wall positions. The waves were plunging but hit the wall before the overhanging part would collapse at the beach. Since the walls were located at two different positions the impact acted at different stages in the breaking process.

A first comparison between the laboratory experiments and Navier-Stokes solver is presented in figure 3. This shows a comparison between a breaking wave at the beach without any vertical wall. As mentioned earlier, a preliminary simulation was performed to support the experimental design - especially with the choice of wall locations. Two different types of impact were generated: flip-through breaking and perfect breaking. W1 was in a position such that the water depth was larger and a flip-through type of impact acted on the wall. When the wall (W2) was moved closer to the shoreline, the solitary wave was at a later stage in the breaking process, and less water was stored up in front of the wave and a vertical front hit the wall with smaller bubbles captured. In the literature this is referred to as perfect breaking by e.g Hattori *et al.* (1994).

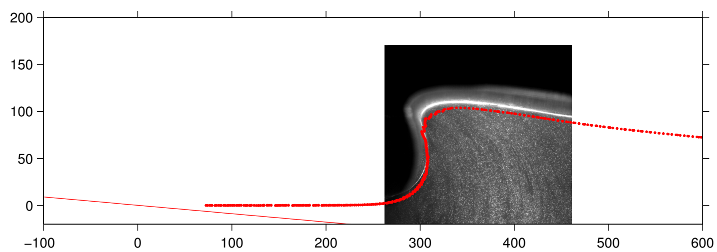

Figure 3: A comparison between an image from the PIV recording and the Navier-Stokes solver; free surface.

The flip-through case has no air entrapment and is a perfect case for the incompressible Navier-Stokes solver. In Figure 4, the free-surface evolution from the VOF model is shown with a nondimensionalized timestep ($t\sqrt{g/h}$) of 0.33. It starts in the left panel from top with increasing time downwards with the solitary wave propagating from right to left in each panel. The overturning begins as the solitary wave propagates closer to the wall. At impact, the toe of the wave (the free surface at the beach and wall) is beginning to move vertically and oppose the overturning of the crest of the wave. This is very similar to what is described in Jensen *et al.* (2003) for a large amplitude solitary wave entering a steep beach. The runup is as expected in these figures - a more interesting feature is in the rundown. At the beach, when the wave is propagating away from the wall, a crater is created and the wave is collapsing backwards. This feature is also observed in the images from the high-speed recordings (images not shown).

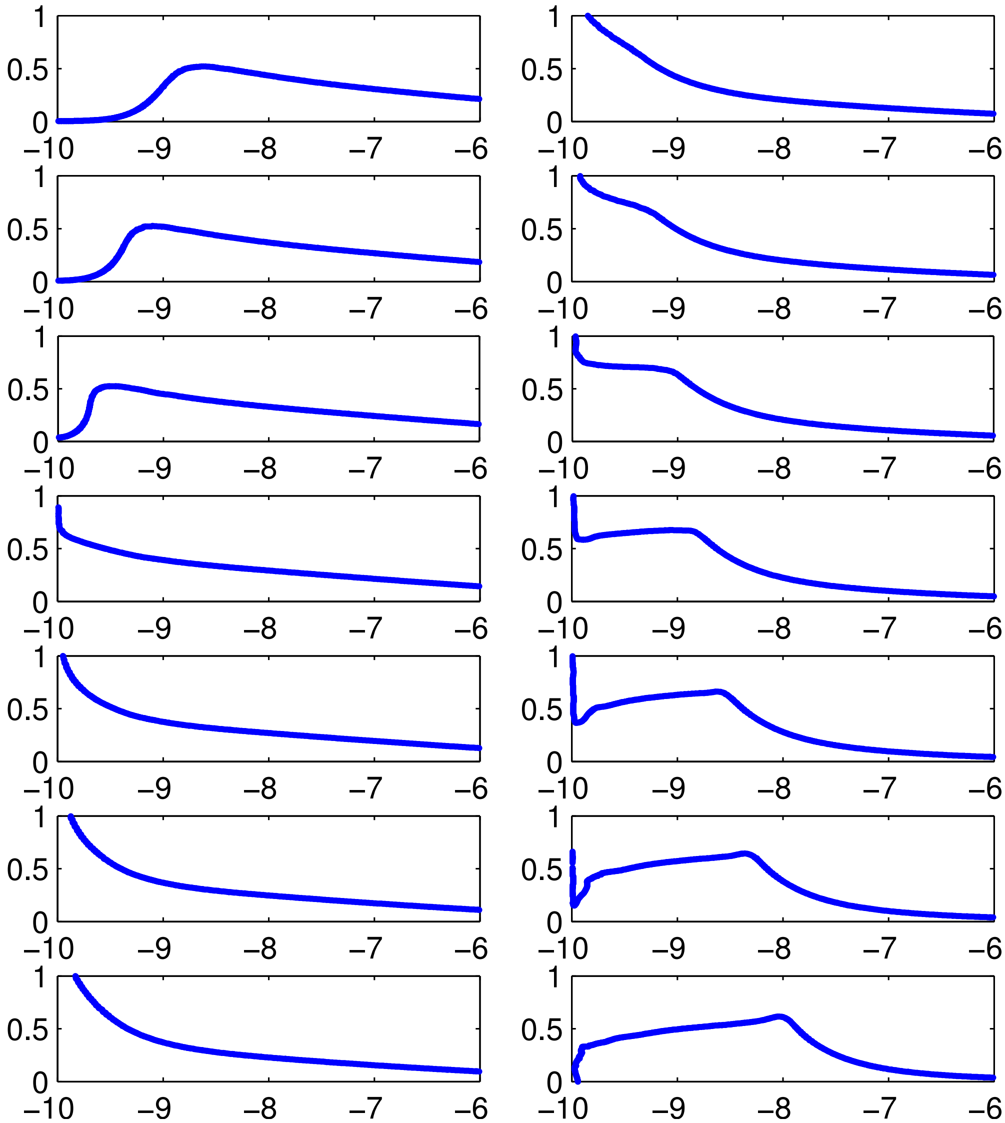

(a) Runup (b) Rundown

Figure 4: Surface profiles from NS3 simulations for the flip-through breaking case. Nondimensional time $t\sqrt{g/h}$ - 35 : 0.33 : 40. The horizontal and vertical axis are scaled by the depth (x/h and y/h).

In Figure 5, raw PIV images are presented with the vector field overlaid. The left panel shows the wave when the front is starting to accelerate along the wall. A jet is formed along the wall and the flip-through is already ended after only a few hundredths of a second. The right panel show the velocity field when maximum pressure is reached. The runup and rundown is very similar to the numerical simulations shown in Figure 4. The collapsing backward feature gives rise to a second pressure peak, see Figure 6. In this figure, both pressure measurements and simulations are displayed. A vertical mean is calculated from the numerical pressure calculations. First runup gives an experimental maximum of $P/\rho gh = 1.1$ for the first pressure peak, with the numerical value being 10% higher. The presence of the second peak is clearly resolved in both the experiment and numerical simulation. It should be noted that the numerical simulation is able to capture both the phase and the magnitude of the impact and also reveal details on the second pressure peak observed and measured in the experiments.

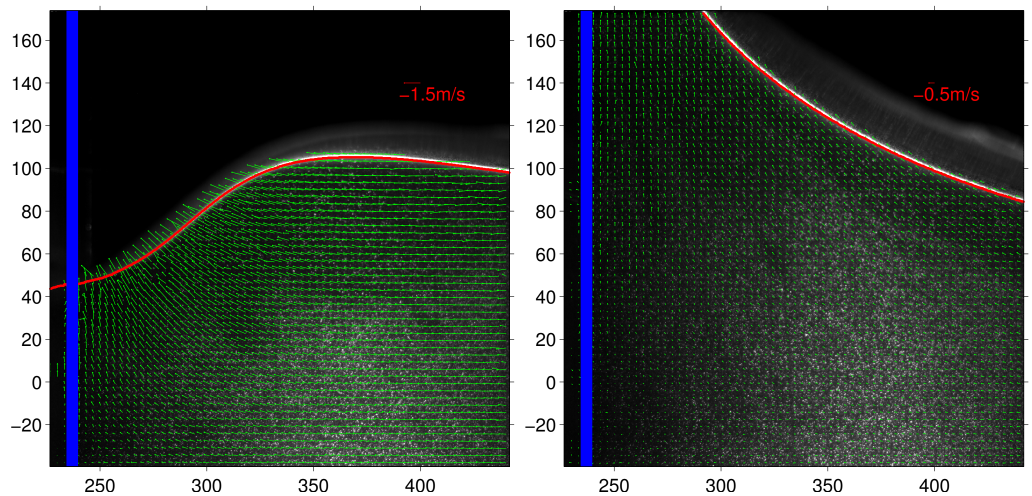

(a) 5.05 s (b) 5.22 s

Figure 5: PIV velocity fields for flip-through breaking. The blue line shows the location of the vertical wall (W1).

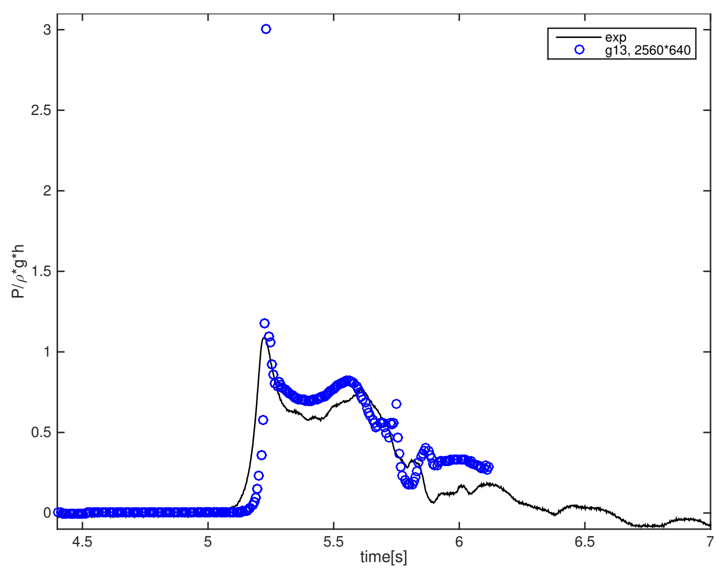

Figure 6: Pressure distribution at the vertical wall (position W1) compared with NS-VOF simulations for flip-through breaking. Rise time: $\Delta t = 0.17s$

In the second set of experiments, the wall was moved closer to the shoreline (W2) to give the wave more time to overturn and a more violent event would occur. The solitary wave was later in the breaking process when it approached the wall. The overturning had come to a later stage in the process and the jet along the wall was too late to overcome the steepening and overturning crest. The vertical front hit the wall at the same time and small bubbles were trapped between the wall and the fluid. This is, as mentioned earlier, referred to a perfect breaking and will maybe give rise to a maximum pressure peak in the recordings. When more air is caught in a pocket close to the wall, the magnitude of the peak pressure will decrease and the pressure rise time will increase. This is reported by, Hattori *et al.* (1994) and Chan & Melville (1988). This case is not simulated by the numerical model, because the simulations broke down when the wave reached the wall, but experimental results are shown. In Figure 7, the velocity field is presented. The left panel shows the breaking wave close to the wall. At the wall, the free surface is starting to move upwards and a jet similar to the flip-through is formed. However, herein the velocities in the crest of the wave are much larger at this stage of the breaking process compared to the wave speed and the vertical front hits the wall, as shown in the right panel in Figure 8.

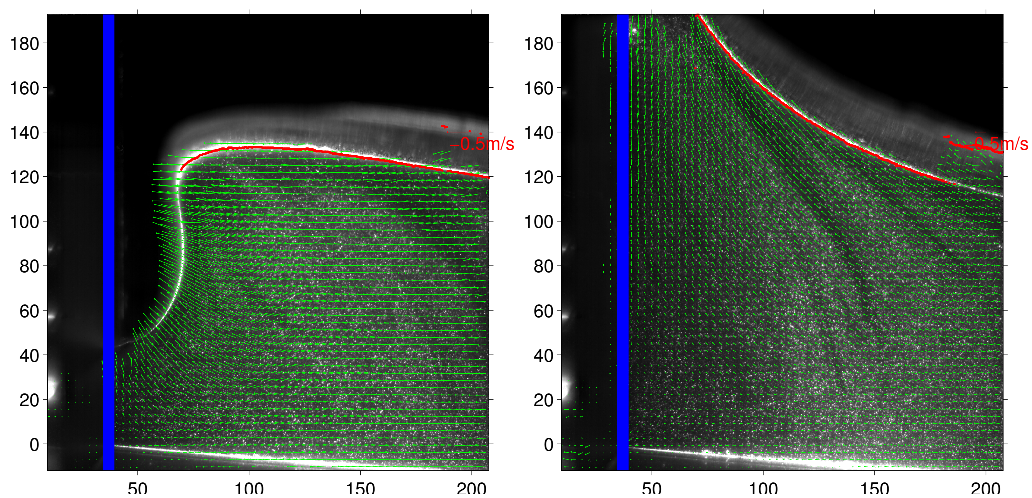

(a) 5.20 s

(b) 5.28 s

Figure 7: PIV velocity fields for perfect breaking. The blue shows the position of the vertical wall (W2).

This impact lasts only a few hundreds of a second. The wave is entering the wall at $t = 5.20$ s, impact at 5.22 s and the wave is running up along the wall at $t = 5.28$ s (as shown in Figures 7 and 8).

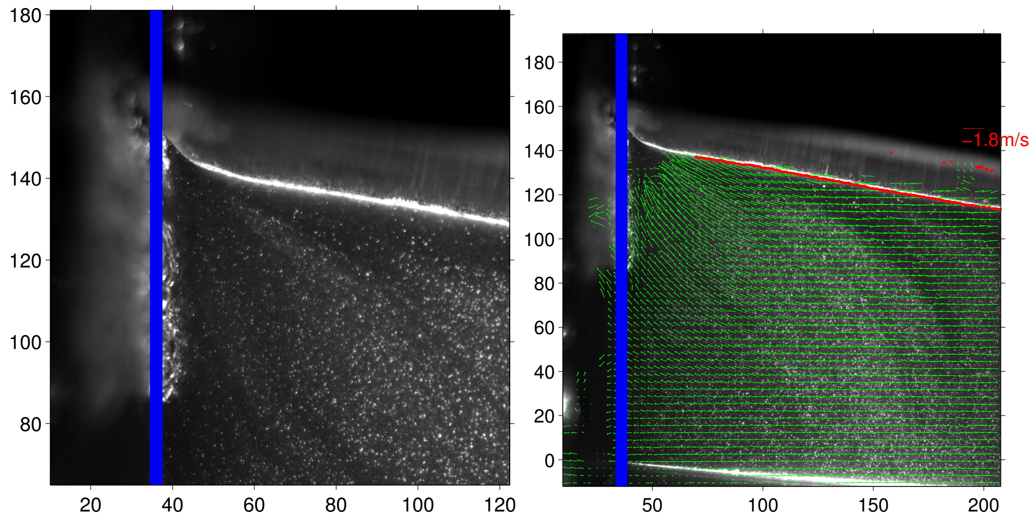

(a) 5.22 s

(b) 5.22 s

Figure 8: PIV velocity fields for violent wave impact (perfect breaking). Left: Image of close up of impact. Right: Raw image and PIV vector field for $t = 5.2$ s. The blue line is the vertical wall (W2).

Results from all three pressure gauges are presented in Figure 9. After the impact, the pressure increases quite rapidly and a maximum of approximately $P/\rho gh = 1.6$ is reached. The rundown is similar to the time evolution of the pressure shown in Figure 6.

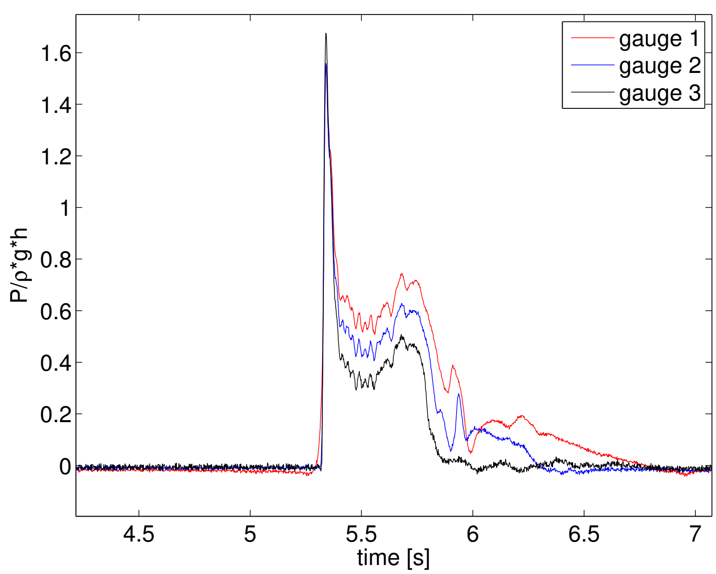

Figure 9: Pressure distribution at the vertical wall (position W2). Rise time: $\Delta t = 0.06s$

The difference between the flip-through and perfect breaking is clear when the kinematics/dynamics are compared. The kinematics of the pre-impact and post-impact were similar. It is when the front face of the wave approached the wall that the difference in impact occurred. Both events produced a strong jet when the toe reached the wall. However, since the wall was moved closer to shore for position W2, the wave had more time to develop a plunging breaker, which acted to suppress the jet along the wall. This is also noticeable when Figures 6 and 9 are compared. Maximum pressure was reached for a much shorter duration for the plunging breaker (Figure 9) than the flip-through breaker (Figure 6), with rise times of $\Delta t = 0.06s$ and $0.17s$ respectively. Furthermore, more oscillations were observed in the pressure recordings for the plunging break (Figure 9). In both breaking types, the second pressure peak was observed due to the crater and the backward collapsing wave.

4 Concluding remarks

Wave impact on a vertical wall has been investigated. A large amplitude solitary wave was generated and was shoaling on a beach before it impacted a wall. Two wall positions were used and mounted on the beach. Furthermore, since the wave impacted the wall at different stages in the breaking process, two different events were occurring. When the wall was located in deeper water, a flip-through phenomenon was observed, where the front face of the wave was moving rapidly vertical due to a jet that was formed at the crossing between the beach and the wall. Both kinematics and pressures were measured and compared with numerical simulations. Similar features were seen in both experiments and simulations. When the wall was moved closer onshore, a more vertical front was impacting the wall. A small amount of air was entrained in the impact and a fast rise of the pressure peak was observed. In the literature this is referred to as a perfect breaker and gives rise to a peak pressure when a wave is violently impacting on a vertical wall. If the wave is overturning before it is impacting on a vertical wall, more air is captured when the wave close around. In this case, less pressure is reported in both theoretical and experimental studies (e.g. Peregrine (2003)).

For both cases a pronounced double pressure peak was observed in the measurements. The time duration for both peaks are larger than the time the solitary wave needs to runup and rundown on the wall. High speed imagery and high resolution numerical simulation reveal that this is caused by a back collapsing wave that fills the crater that is created by the rundown. A second wave is breaking in opposite direction of the traveling wave that is going offshore. This second collapsing breaking wave is the source that created the second pressure peak.

Acknowledgments
The author is deeply indebted to Svein Vesterby and Arve Kvalheim at UiO for providing technical expertise, and to Graigory Sutherland for comments and advice that significantly improved the manuscript. Furthermore, the author would like to acknowledge DHI for the permission to use the software NS3.

References

BULLOCK, G., OBHRAI, C., PEREGRINE, D. & BREDMOSE, H. 2007 Violent breaking wave impacts. part 1: Results from large-scale regular wave tests on vertical and sloping walls. *Coastal Eng.* **54**, 602–617.

CHAN, E. S. & MELVILLE, W. K. 1988 Deep-water plunging wave pressures on a vertical plane wall. *Proc. R. Soc. Lond. A* **417**, 95–113.

CHELLA, M. A., BIHS, H., MYRHAUG, D. & MUSKULUS, M. 2017 Breaking solitary waves and breaking wave forces on a vertically mounted slender cylinder over an impermeable sloping seabed. *Journal of Ocean Engineering and Marine Energy* **3** (1), 1–19.

COKELET, E. D. 1977 Breaking waves. *Nature* **267**, 769–774.

CUOMO, G., ALLSOP, W., BRUCE, T. & PEARSON, J. 2010 Breaking wave loads at vertical seawalls and breakwaters. *Coastal Eng.* **57**, 424–439.

DAO, M. H., XU, H., CHAN, S., E. & TKALICH, P. 2013 Modelling of tsunami-like wave run-up, breaking and impact on a vertical wall by sph method. *Natural Hazards and Earth System Sciences* **13** (12), 3457–3467.

GUILCHER, P. M., BROSSET, L., COUTY, N. & TOUZE, D. L. 2012 Simulations of breaking wave impacts on a rigid wall at two different scales with a two phases fluid compressible sph model. In *In Proceedings of 22nd International Offshore and Polar Engineering Conference (ISOPE), Rhodes, Greece*.

GUILCHER, P. M., OGER, G., BROSSET, L., JACQUIN, E., GRENIER, N. & TOUZE, D. L. 2010 Simulation of liquid impacts with a two-phase parallel sph model. In *In Proceedings of 20th International Offshore and Polar Engineering Conference (ISOPE) , Beijing, China*.

HATTORI, M., ARAMI, A. & YUI, T. 1994 Wave impact pressure on vertical walls under breaking waves of various types. *Coastal Eng.* **22**, 79–114.

HIRT, C. W. & NICHOLS, B. D. 1981 Volume of fluid (VOF) method for the dynamics of free boundaries. *J. Comput. Phys.* **39**, 201 – 225.

JENSEN, A., MAYER, S. & PEDERSEN, G. K. 2005 Experiments and computation of onshore breaking solitary waves. *Meas. Sci. Technol.* **16**, 1913–1920.

JENSEN, A., PEDERSEN, G. K. & WOOD, D. J. 2003 An experimental study of wave run-up at a steep beach **486**, 161–188.

KAWAMURA, T., MAYER, S., GARAPON, A. & SØRENSEN, L. 2002 Large eddy simulation of a flow past a free surface piercing circular cylinder. *Journal of Fluids Engineering* **124**.

KIMMOUN, O., SCOLAN, Y., Y. M. & MALENICA, S., S. 2009 Fluid structure interactions occurring at a flexible vertical wall impacted by a breaking wave. In *In the Nineteenth International Offshore and Polar Engineering Conference (ISOPE)*.

LONGUET-HIGGINS, M. S. & COKELET, E. D. 1976 The deformation of steep surface waves on water. I. A numerical method of computation. *Phil. Trans. Roy. Soc. London, A* **350**, 1–26.

LUGNI, C., BROCCHINI, M. & FALTINSEN, O. M. 2006 Wave impact loads: The role of the flip-through. *Physics of fluids* **18**, 122101.

MAYER, S., GARAPON, A. & SØRENSEN, L. 1998 A fractional step method for unsteady free surface flow with applications to non-linear wave dynamics. *Int. J. Num. Meth. Fluids* **28**, 293–315.

MAYER, S. & MADSEN, P. A. 2000 Simulations of breaking waves in the surf zone using a Navier-Stokes solver. In *ICCE 96, 25'th Coastal Engineering Conference*. Sydney, Australia.

MO, W., JENSEN, A. & LIU, P. L. 2013 Plunging solitary wave and its interaction with a slender cylinder on a sloping beach. *Ocean Engineering* **74** (1), 48–60.

OUMERACI, H., KLAMMER, P. & PARTENSCKY, H. W. 1993 Classification of breaking wave loads on vertical structures. *Journal of Waterway, Port, Coastal and Ocean Engineering* **119**, 381–397.

PEREGRINE, D. H. 1983 Breaking waves on beaches. *Ann. Rev. Fluid Mech.* .

PEREGRINE, D. H. 2003 Water-wave impact on walls. *Ann. rev. of Fluid Mech.* **35**, 23–43.

PLUMERAULT, L.-R., ASTRUC, D. & MARON, P. 2012 The influence of air on the impact of a plunging breaking wave on a vertical wall using a multifluid model. *Coastal Eng.* **62**, 62–74.

SCOLAN, Y. 2010 Some aspects of the flip-through phenomenon: A numerical study based on the desingularized technique. *Journal of Fluids and Structures* (26), 918–953.

SMITH, L., JENSEN, A. & PEDERSEN, G. 2017 Investigation of breaking and non-breaking solitary waves and measurements of swash zone dynamics on a 5 beach. *Coastal Engineering* **120**, 38–46.